

---

# Clinical Usefulness of $^{18}\text{F}$ -FDG PET in Nasopharyngeal Carcinoma Patients with Questionable MRI Findings for Recurrence

Ng Shu-Hang, MD<sup>1</sup>; Joseph Chang Tung-Chieh, MD, MSc<sup>2</sup>; Chan Sheng-Chieh, MD<sup>3</sup>; Ko Sheung-Fat, MD<sup>1</sup>; Wang Hung-Ming, MD<sup>4</sup>; Liao Chun-Ta, MD<sup>5</sup>; Chang Yu-Chen, MD<sup>3</sup>; Wu-Jyh Lin, PhD<sup>6</sup>; Fu Ying-Kai, PhD<sup>6</sup>; and Yen Tzu-Chen, MD, PhD<sup>3</sup>

<sup>1</sup>Department of Diagnostic Radiology, Chang Gung Memorial Hospital Linkou Medical Center, Taoyuan, Taiwan; <sup>2</sup>Department of Radiation Oncology, Chang Gung Memorial Hospital Linkou Medical Center, Taoyuan, Taiwan; <sup>3</sup>Department of Nuclear Medicine, Chang Gung Memorial Hospital Linkou Medical Center, Taoyuan, Taiwan; <sup>4</sup>Department of Medical Oncology, Chang Gung Memorial Hospital Linkou Medical Center, Taoyuan, Taiwan; <sup>5</sup>Department of Otorhinolaryngology, Chang Gung Memorial Hospital Linkou Medical Center, Taoyuan, Taiwan; <sup>6</sup>Institute of Nuclear Energy Research, Taoyuan, Taiwan

---

It has been reported that  $^{18}\text{F}$ -FDG PET is highly sensitive for the detection of recurrent head-and-neck cancer. The objective of our prospective study was to validate the ability of this technique to detect the presence of tumors in primary, nodal, and distant sites as well as to assess its overall clinical usefulness in patients with questionable MRI findings for residual or recurrent nasopharyngeal carcinoma (NPC). **Methods:** From January 2002 to October 2003, a group of 37 NPC patients whose postradiation follow-up MRI examination showed questionable residual or recurrent disease was assessed with  $^{18}\text{F}$ -FDG PET.  $^{18}\text{F}$ -FDG PET was interpreted visually. Disease at primary, nodal, and distant sites was assessed. The final diagnosis was confirmed histopathologically or with clinical and imaging follow-up of at least 6 mo. **Results:** Our results showed that the sensitivity and specificity of  $^{18}\text{F}$ -FDG PET for the detection of recurrent NPC were 91.6% and 76.0%, respectively, at the primary site; 90.0% and 88.9%, respectively, at nodal sites; and 100% and 90.6%, respectively, at distant sites. The overall sensitivity and specificity were 89.5% and 55.6%, respectively. Among the 37 patients,  $^{18}\text{F}$ -FDG PET added significant information to the MRI findings in 18, including offering true-negative findings in 10, revealing unexpected small metastatic adenopathy in 3, and disclosing distant metastatic foci in 5. **Conclusion:**  $^{18}\text{F}$ -FDG PET is highly sensitive and moderately specific for the detection of recurrent NPC in patients with questionable MRI findings. Overall,  $^{18}\text{F}$ -FDG PET appears to add significant information to MRI findings in about half of the NPC patients whose MRI examination shows questionable tumor recurrence.

**Key Words:** nasopharyngeal carcinoma; MRI;  $^{18}\text{F}$ -FDG PET; tumor recurrence

**J Nucl Med 2004; 45:1669–1676**

**N**asopharyngeal carcinoma (NPC) is a malignant tumor of epidermoid origin distributed mainly among well-defined ethnic populations. The highest incidence of NPC is found in the people of Southern China and Hong Kong and is followed by the incidence in the people of Singapore and Taiwan and in Chinese Americans (1–4). The mainstay of treatment is radiotherapy, but chemotherapy is also needed in advanced disease (5,6). Radiotherapy can cause various tissue changes and considerable anatomic distortion, which hinder the recognition of residual or recurrent disease by clinical examination and conventional anatomic imaging (7–9).

Although flexible endoscopy is generally more sensitive than imaging for identifying mucosal recurrence (10), post-radiation mucositis, crusting, or varying degrees of trismus may hamper endoscopy. MRI, by virtue of its high contrast resolution and multiplanar capability, is currently the preferred conventional imaging modality, rather than CT, in posttherapy surveillance of NPC (11–16). However, MRI still presents some difficulty in differentiating postradiation changes from residual or recurrent tumor. Soft tissue seen in the irradiated nasopharynx or neck on MRI always poses a diagnostic question of whether the lesion harbors viable tumor (10–12,14,15). This difficult problem is generally managed by biopsy or by a wait-and-see policy with serial clinical or imaging follow-up examinations. However, biopsy of previously irradiated tissues cannot be done with impunity as it carries a significant risk of bleeding and infection, whereas a wait-and-see policy may result in disease progression and delayed salvage treatment.

PET is a functional imaging technique that provides information about tissue metabolism. PET with  $^{18}\text{F}$ -FDG has shown promise in the detection of head-and-neck malignancy by identifying regions of accelerated glucose metabolism (17). It has also proved to be useful in distinguish-

---

Received Jan. 13, 2004; revision accepted Apr. 23, 2004.  
For correspondence or reprints contact: Yen Tzu-Chen, MD, PhD, Department of Nuclear Medicine, Chang Gung Memorial Hospital, Linkou Medical Center, 5 Fu-Shin St, Kueishan, Taoyuan 333, Taiwan.  
E-mail: yen1110@adm.cgmh.org.tw

ing residual or recurrent tumors from postradiation changes, with sensitivities ranging from 88% to 100% and specificities ranging from 64% to 100% (18–22). To our knowledge, there have been only 4 reports comparing the usefulness of  $^{18}\text{F}$ -FDG PET and CT in NPC, of which one showed that  $^{18}\text{F}$ -FDG PET was more accurate than CT in identifying cervical nodal metastasis in pretreated NPC (23) whereas the other 3 showed extremely high sensitivity (100%) for  $^{18}\text{F}$ -FDG PET in detecting recurrent NPC at the primary site (24–26). Two later studies compared the feasibility of  $^{18}\text{F}$ -FDG PET and MRI for detecting recurrent NPC at the primary site (27,28), and both also showed a sensitivity of 100%. However, the usefulness of  $^{18}\text{F}$ -FDG PET in detecting recurrent NPC at nodal and distant sites has not been reported. In clinical practice, questionable MRI findings are not uncommonly encountered in posttherapy surveillance of NPC, and a thorough assessment of disease status in primary, nodal, and distant sites is important for appropriate diagnosis and treatment. Accordingly, we conducted a prospective study to assess the usefulness of  $^{18}\text{F}$ -FDG PET in solving such clinical problems of NPC patients with questionable MRI findings.

## MATERIALS AND METHODS

### Patients

This study was conducted from January 2002 to October 2003 under the approval of the Institutional Review Board of our hospital, with written informed consent obtained from all enrolled subjects. The criterion for eligibility was the presence of questionable MRI findings for recurrence of NPC during periodic surveillance. Questionable MRI findings were defined, using morphologic criteria, as findings that were beyond those expected after radiotherapy, either unequivocal or suggestive of residual or recurrent NPC.  $^{18}\text{F}$ -FDG PET was performed within 2 wk of the MRI study. The lesions were confirmed by histopathology or by a follow-up—both clinical and cross-sectional imaging—of at least 6 mo.

### MRI

In our hospital, most patients with NPC are examined with MRI under a standard protocol. Baseline MRI is performed 3–4 mo after therapy and then every 6 mo for the first 2 y. Thereafter, follow-up MRI is performed annually. An additional MRI examination is done whenever there is suspicion of recurrent disease based on clinical or previous imaging assessment. MRI was performed with a 1.5-T unit (Vision; Siemens) using spin-echo technique. All patients underwent MRI before and after injection of gadolinium diethylenetriaminepentaacetic acid (DTPA). A head coil was used to examine the region from the superior margin of the temporal lobe to the level of the hyoid bone. A neck coil was then used to examine the rest of the neck and the supraclavicular fossa. Unenhanced T1-weighted images were acquired in the sagittal and axial planes with a spin-echo 500/20 (repetition time/echo time, in milliseconds) sequence, a 20-cm field of view, and a  $192 \times 256$  matrix. Axial and coronal T2-weighted fat-suppressed fast-spin-echo images (3000/85 [effective], 16–echo train length) were also obtained. Section thickness was 5 mm with a 1-mm interslice gap in the axial projection and 4 mm with a 1-mm gap in

the sagittal and coronal projections. After gadolinium DTPA injection at a dose of 0.1 mmol/kg of body weight, T1-weighted fat-suppressed axial, sagittal, and coronal sequences were obtained sequentially, with parameters similar to those used before the gadolinium DTPA injection.

### $^{18}\text{F}$ -FDG PET

The  $^{18}\text{F}$ -FDG used for the PET studies was produced by the Institute of Nuclear Energy Research of Taiwan. All  $^{18}\text{F}$ -FDG PET scans were acquired with a dedicated PET system (ECAT EXACT HR+; Siemens-CTI), using a 4.5-mm full width at half-maximum and a transaxial field of view of 15 cm. All patients had been fasting for at least 6 h before undergoing PET. After intravenous injection of 370 MBq (10 mCi) of  $^{18}\text{F}$ -FDG, the patients were kept at rest in a quiet, dimly lit room for at least 40 min. Talking, walking, or other physical activities were avoided to reduce muscle uptake.

Dual-phase  $^{18}\text{F}$ -FDG PET was performed on all patients while they lay supine along the central axis of the PET table. Initially, 7 sequential images were obtained from the head to the upper thigh, requiring 56 min using a 2-dimensional mode. After 3 h, the second-phase  $^{18}\text{F}$ -FDG PET scan was acquired from the neck to the head, requiring a further 25 min. Transmission scanning with 3  $^{68}\text{Ge}/^{68}\text{Ga}$  rod sources was performed for attenuation correction immediately after  $^{18}\text{F}$ -FDG administration. Reconstruction of transmission and emission scans used accelerated maximum-likelihood reconstruction. Maximum-intensity-projection images were viewed on a workstation that allowed simultaneous viewing of coronal, sagittal, and transverse planes as well as a 3-dimensional rotation projection. The anatomic references for whole-body PET were the apex of the heart; the circumferences of the liver, kidney, and urinary bladder; and the bone marrow of the vertebral column. The standardized uptake value (SUV) was yielded by analysis of the region of interest. The region of interest was placed on the emission image at the area of increased  $^{18}\text{F}$ -FDG uptake. The edge of the region of interest was placed at the contour for 75% of peak counts.

### Image Interpretation and Analysis

Three experienced nuclear medicine physicians interpreted the  $^{18}\text{F}$ -FDG PET studies individually by visual inspection of the scans in transverse, sagittal, and coronal sections. They had no knowledge of the MRI findings. The SUV of the  $^{18}\text{F}$ -FDG uptake was used as an accessory reference. Foci of increased  $^{18}\text{F}$ -FDG uptake were evaluated and the uptake scored on a 5-point scale: 0 = no abnormal uptake, 1 = benign, 2 = probably benign, 3 = probably malignant, and 4 = definitely malignant (29). A checklist of the distributions of tumor extension, nodal spread, and distant metastasis was recorded accordingly. Both grade 3 and grade 4 were considered to indicate residual or recurrent NPC. Any initial difference of opinion was resolved by consensus.

### Outcome Determination and Data Analysis

The  $^{18}\text{F}$ -FDG PET, MRI, and clinical findings were discussed jointly by the NPC research team, consisting of the nuclear medicine physicians, head-and-neck radiologists, otolaryngologists, medical oncologists, and radiation oncologists. Endoscopic biopsy, ultrasonographically guided fine-needle aspiration, or CT-guided biopsy was performed, if possible, for any lesions suspected of malignancy. If biopsy of the lesion of interest was not feasible or yielded a negative result, close clinical and imaging

follow-up was pursued. Relevant information was obtained from thorough review of all relevant records and from discussion among the members of the research team. Then, <sup>18</sup>F-FDG PET results were classified as true positive, true negative, false positive, or false negative. To assess the efficacy of <sup>18</sup>F-FDG PET, we calculated the sensitivity, specificity, positive predictive value, negative predictive value, and accuracy of this technique.

## RESULTS

Table 1 shows clinical data for the 37 NPC patients enrolled in this study. Thirteen were female and 24 were male, with ages ranging from 16 to 76 y (mean, 47.2 y). The T-stages of their NPC at initial presentation were T1 in 7

patients, T2 and T3 in 9 patients each, and T4 in 12 patients. The nodal stages were N0 in 11 patients, N1 in 10 patients, N2 in 14 patients, and N3 in 2 patients. All patients received intensity-modulated radiation therapy, with additional concurrent chemotherapy for 25 patients and additional intracavity radiotherapy for 7 patients. The average period from the completion of primary treatment to the time of the <sup>18</sup>F-FDG PET study was 14.1 ± 22.9 mo (range, 3.7–112.6 mo). Of the 37 patients, 19 had residual (*n* = 4) or recurrent (*n* = 15) tumor, and 18 had benign changes. Of the 19 cases of residual or recurrent NPC, 5 occurred at the primary site, 4 at the regional nodes, 2 at distant sites, 5 at both the primary and nodal sites, 2 at both the primary and distant

**TABLE 1**  
Clinical Information and PET Results for 37 NPC Patients with Questionable MRI Findings for Residual or Recurrent Disease

Patient no.	Age (y)	Sex	Initial stage	Treatment mode	Interval* (m)	PET result			
						Primary	Node	Distance	Overall
1	40	M	T4 N2 M0	IMRT + CC	6.8	FP	TN	TN	FP
2	49	M	T4 N0 M0	IMRT + CC	4.2	TN	TN	TN	TN
3	38	F	T2 N2 M0	IMRT + CC	3.9	FP	TN	TN	FP
4	49	M	T3 N0 M0	IMRT + CC	12.7	TP	TN	TN	TP
5	53	M	T1 N2 M0	IMRT + BB	14.3	FP	TN	TN	FP
6	60	M	T1 N0 M0	IMRT + BB	24.2	FP	TN	TN	FP
7	44	F	T2 N1 M0	IMRT	12.5	FN	TN	TN	FN
8	42	M	T3 N1 M0	IMRT + CC	23.5	TP	TN	TP	TP
9	44	M	T3 N2 M0	IMRT + CC	3.8	TN	FN	TN	FN
10	59	F	T2a N1 M0	IMRT	4.9	TN	TP	TN	TP
11	47	M	T1 N2 M0	IMRT + BB	4.3	TN	FP	TN	FP
12	64	F	T2 N1 M0	IMRT	6.8	TN	TP	TN	TP
13	70	M	T2 N1 M0	IMRT	112.6	TN	TN	TN	TN
14	34	M	T4 N2 M0	IMRT + CC	3.7	TP	TP	TN	TP
15	41	M	T3 N2 M0	IMRT + CC	3.9	FP	TN	TP	TP
16	49	M	T3 N0 M0	IMRT + CC	3.7	FP	TN	TN	FP
17	43	F	T1 N2 M0	IMRT + BB	3.8	TN	TP	TP	TP
18	44	F	T2b N2 M0	IMRT + CC	15.9	TP	TP	TN	TP
19	59	M	T4 N0 M0	IMRT + CC	3.7	TN	TN	TN	TN
20	50	M	T3 N0 M0	IMRT + CC	12.2	TP	TN	TP	TP
21	29	M	T3 N1 M0	IMRT + CC	3.9	TN	TN	FP	FP
22	35	M	T4 N2 M0	IMRT + CC	13.1	TP	TN	TN	TP
23	16	F	T4 N2 M0	IMRT + CC	4.2	TN	TN	TN	TN
24	76	M	T4 N0 M0	IMRT + CC	3.9	TN	TN	TN	TN
25	45	F	T4 N3 M0	IMRT + CC	10.5	TP	TP	FP	TP
26	51	F	T1 N0 M0	IMRT + BB	90.2	TP	FP	FP	TP
27	40	M	T3 N1 M0	IMRT + CC	3.7	TN	FP	TN	FP
28	45	F	T2b N2 M0	IMRT + CC	13.9	TN	TN	TN	TN
29	45	F	T2b N0 M0	IMRT	3.9	TP	TP	TN	TP
30	43	M	T1 N0 M0	IMRT + BB	39.6	TN	TP	TN	TP
31	38	M	T1 N1 M0	IMRT + BB	3.8	TN	TN	TN	TN
32	40	M	T4 N0 M0	IMRT + CC	31.2	TP	TN	TN	TP
33	47	F	T2b N2 M0	IMRT + CC	3.8	TN	TN	TN	TN
34	42	F	T4 N1 M0	IMRT + CC	3.9	TN	TN	TN	TN
35	66	M	T4 N1 M0	IMRT + CC	4.3	TN	TN	TN	TN
36	63	M	T3 N3 M0	IMRT + CC	3.8	TP	TP	TN	TP
37	48	M	T4 N2 M0	IMRT + CC	3.7	TN	TN	TP	TP

\*Between the complement of therapy and <sup>18</sup>F-FDG PET.

IMRT = intensity-modulated radiation therapy; IMRT + CC = IMRT with concurrent chemotherapy; IMRT + BB = IMRT with brachytherapy boost; TP = true positive; FP = false positive; TN = true negative; FN = false negative.

**TABLE 2**  
<sup>18</sup>F-FDG PET Results for 37 NPC Patients for Whom MRI Showed Questionable Findings for Residual or Recurrent Disease

Site	TP	TN	FP	FN	Sensitivity (%)	Specificity (%)	PPV (%)	NPV (%)	Accuracy (%)
Primary	11	19	6	1	91.6 (61.5–99.8)	76.0 (54.9–90.6)	64.7 (38.3–85.8)	95.0 (75.1–99.9)	81.1 (64.8–92.0)
Regional node	9	24	3	1	90.0 (55.5–99.8)	88.9 (70.8–97.7)	75.0 (42.8–94.5)	96.0 (79.7–99.9)	89.2 (74.6–97.0)
Distant	5	29	3	0	100	90.6 (75.0–98.0)	62.5 (24.5–91.5)	100	91.9 (78.1–98.3)
Overall	17	10	8	2	89.5 (66.9–98.7)	55.6 (30.8–78.5)	68.0 (46.5–78.5)	83.3 (51.6–98.0)	72.9 (55.9–86.2)

TP = true positive; TN = true negative; FP = false positive; FN = false negative; PPV = positive predictive value; NPV = negative predictive value.

Ranges in parentheses are 95% CIs.

sites, and 1 at both nodal and distant sites. <sup>18</sup>F-FDG PET correctly detected 17 residual or recurrent tumors and affirmed 10 true-negative cases. However, 8 false-positive and 2 false-negative results were also found. The sensitivity, specificity, positive predictive value, negative predictive value, and accuracy of <sup>18</sup>F-FDG PET are listed in Table 2. The SUVs of the early and delayed phases of <sup>18</sup>F-FDG PET in areas of positive uptake are listed in Table 3. At the primary site, the mean value of the SUV of the true-positive lesions was significantly higher than the corresponding value of the false-positive lesions (8.77 vs. 3.39; *P* = 0.002). However, the ranges of the SUVs for the true-positive and false-positive lesions were wide, being 4.34–13.8 and 1.63–5.09, respectively. The mean values of the SUV for the true-positive lesions were also higher than those for false-positive lesions at the regional nodes (4.46 vs. 2.71) and distant sites (4.42 vs. 2.67), but the difference was not significant. On the other hand, the mean values of the SUV obtained at 3 h were lower than those at 40 min in both the true-positive and the false-positive lesions at the

primary site and in the true-positive lesions at the regional nodes. Only false-positive lesions at the regional nodes exhibited higher mean values of SUV at 3 h than at 40 min. There was no significant difference in retention index between true-positive uptake and false-positive uptake at the 2 scan times in the primary site (–10.99 vs. –7.07; *P* = 0.588) and in the regional nodes (–0.36 vs. 19.01; *P* = 0.094).

#### Primary Site

Seventeen PET scans had positive findings and 20 had negative findings at the primary sites of disease. Eleven of the 17 positives were true positive, with positive biopsy findings. Among these 11 true positives, 3 were considered to be residual NPC because the disease was identified at the first follow-up MRI study and at <sup>18</sup>F-FDG PET studies 4 mo after radiotherapy. Of the 6 positives judged to be false positive (Fig. 1), biopsy of the areas of <sup>18</sup>F-FDG uptake showed inflammatory changes in 4 cases and infection and lymphoid hyperplasia in 1 case each. All 6 cases lacked

**TABLE 3**  
SUV Results at 40 Minutes and at 3 Hours

Site	<i>n</i>	SUV1 (at 40 min)		SUV2 (at 3 h)		RI		<i>P1</i>
		Mean ± SD	Range	Mean ± SD	Range	Mean ± SD	Range	
Primary								
TP	11	8.77 ± 3.4	4.34–13.8	8.01 ± 3.75	3.12–14.04	–10.99 ± 15.74	–46.11–8.56	0.05
FP	6	3.39 ± 1.28	1.63–5.09	3.22 ± 1.48	1.50–5.23	–7.07 ± 9.39	–19.07–3.67	0.227
<i>P2</i>		0.002*		0.01†		0.588		
Regional node								
TP	9	4.46 ± 3.41	2.15–11.9	4.41 ± 3.44	2.41–11.66	–0.36 ± 13.9	–33.75–12.09	0.249
FP	3	2.71 ± 0.26	2.45 ± 2.96	3.19 ± 0.27	3.0–3.5	19.01 ± 21.4	1.35–42.86	0.8
<i>P2</i>		0.412		0.567		0.094		
Distant								
TP	5	4.42 ± 1.99	2.36–7.69					
FP	3	2.67 ± 0.31	2.40–3.0					
<i>P2</i>		0.191						

\**P* < 0.01.

†*P* < 0.05.

RI = retention index; TP = true positive; FP = false positive; *P1* = paired *t* test comparing SUV1 and SUV2; *P2* = independent *t* test comparing SUV1, SUV2, and RI between TP and FP.

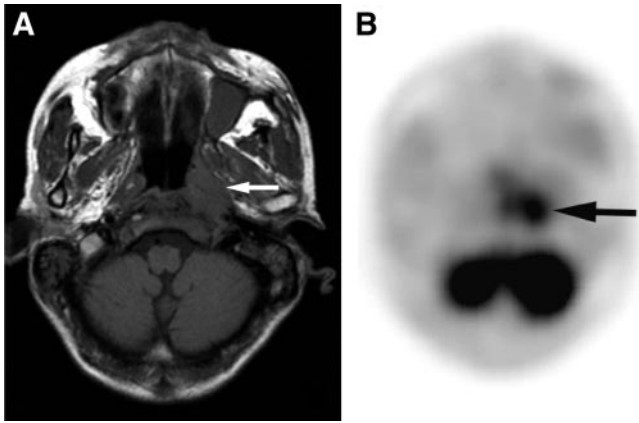


**FIGURE 1.** A 53-y-old man with NPC 14 mo after intensity-modulated radiation therapy and intracavity brachytherapy. (A) Axial T1-weighted MR image shows an irregular mass (arrow) in the left nasopharynx. (B)  $^{18}\text{F}$ -FDG PET image shows a false-positive finding. Histopathologic findings showed acute and chronic inflammation, and follow-up MRI 4 mo later showed regression of the lesion.

evidence of recurrence on clinical and imaging follow-up of more than 6 mo, and 4 showed lesion regression in subsequent follow-up images.

Nineteen of the 20 negative results were considered to be true negative (Fig. 2) based either on the consistent clinical and imaging follow-up findings over a period averaging 16 mo (range, 6–30 mo) ( $n = 13$ ) or on a biopsy specimen that revealed only fibrotic and inflammatory changes ( $n = 6$ ). Only 1  $^{18}\text{F}$ -FDG PET scan—of a patient with mucosal recurrence—had false-negative results. This was confirmed by endoscopic biopsy (Fig. 3).

#### Regional Nodal Disease

Twelve PET scans had positive findings and 25 had negative findings for nodal disease. Nine of the 12 positives

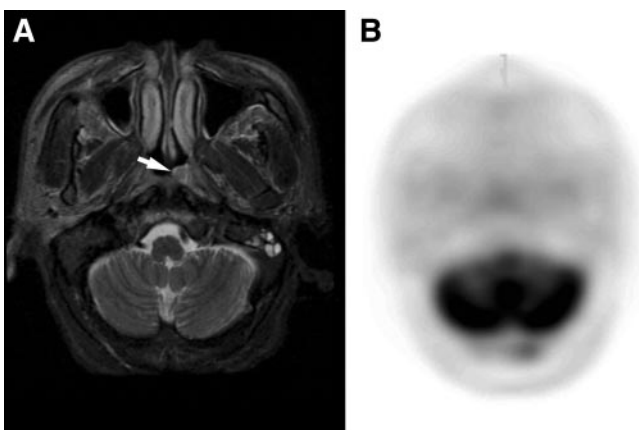


**FIGURE 2.** A 59-y-old man with NPC 16 mo after concurrent chemoradiation therapy. (A) Axial T2-weighted MR image shows an irregular mass (arrow) in the left nasopharynx. (B)  $^{18}\text{F}$ -FDG PET finding is true negative, with the image showing no uptake in the corresponding area. Subsequent biopsy showed this was an inflammatory mass.

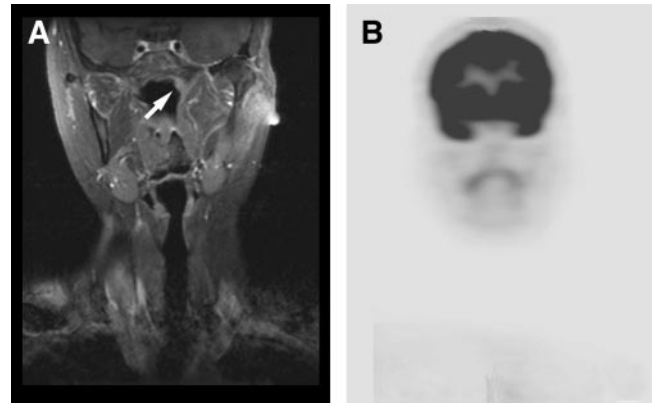


**FIGURE 3.** A 44-y-old woman with NPC 9 mo after intensity-modulated radiation therapy. (A) Coronal contrast-enhanced T1-weighted MR image shows an asymmetric mucosal thickening (arrow) in the left nasopharynx. (B) However, the negative  $^{18}\text{F}$ -FDG PET findings are false, for histopathologic examination showed a recurrent NPC.

were true positive, as confirmed by tissue sampling in 7 patients and by unequivocal clinical and imaging progression in the other 2. Among these 9 true positives, 4 were for patients with residual nodal disease whereas the other 5 were for patients with recurrent adenopathy (Fig. 4). On MRI, the nodes were considered to be equivocal for residual or recurrent nodal disease in 3 patients and to be suggestive of nodal metastasis in another 3. The nodes of the remaining 3 patients were thought to be nonmalignant because of their small size on MRI.

On the other hand, of the 3 results judged to be false positive, 1 showed sinus histiocytosis, 1 showed lymphoid hyperplasia, and 1 showed regression in clinical and imaging follow-up. Twenty-four of the 25 negative results were classified as true negative after clinical and imaging follow-up in 22 patients (range, 6–24 mo; average, 12 mo) and by biopsy in the other 2 patients. On MRI, the nodes were

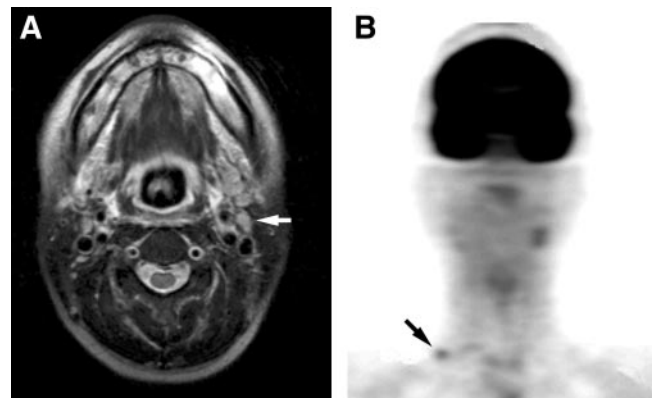


**FIGURE 4.** A 45-y-old woman with NPC 12 mo after intensity-modulated radiation therapy. (A) Axial T2-weighted MR image shows a questionable left-sided high jugular adenopathy (arrow). (B)  $^{18}\text{F}$ -FDG PET scan reveals an additional metastatic node (arrow) in the right supraclavicular fossa in addition to the left-sided high jugular metastatic node.

considered to be equivocal for residual or recurrent nodal disease in 3 patients, suggestive of nodal metastasis in 6, and suggestive of a benign process in 7. In the remaining 8 patients, no visible nodes were seen. The 1 false-negative  $^{18}\text{F}$ -FDG PET result occurred in a patient with a small, residual high jugular node of 0.5-cm diameter, proven through subsequent ultrasonographically guided fine-needle aspiration.

#### Distant Sites

Eight PET scans had positive findings and 29 had negative findings for distant metastases. Five positives were true positive, as confirmed by tissue sampling in 2 patients (sampling in the iliac crest for 1 and in the axillary node for 1) and by obvious clinical and imaging progression in 3 (progression in the lung for 1, in the liver for 1, and in the spine for 1). All these metastatic lesions were clinically occult. In 2 of these 5 patients, distant metastases were found at the initial posttherapy examination 4 mo after radiotherapy and occurred as the sole manifestation of recurrent disease without local recurrence at the primary site or at regional nodes. In another patient,  $^{18}\text{F}$ -FDG PET suggested a single distant metastatic adenopathy in the left perihilar region of the chest, whereas confirmatory chest CT showed that the lesion was in fact a perihilar pulmonary nodule. CT also showed an additional small nodule (about 0.5 cm in diameter) in the right lower lobe (Fig. 5).

On the other hand, 3 results were judged to be false positive, with 1 proven by biopsy (granulomatous adenitis in another axillary node) and 2 by clinical or imaging follow-up (presumed reactive hyperplasia in the mediastinal node for 1 and a posttraumatic effect in the humerus for 1).

#### Overall Assessment

In the overall assessment of residual or recurrent NPC by the counting of all the primary, nodal, and distant sites

together,  $^{18}\text{F}$ -FDG PET showed 17 true positives, 10 true negatives, 2 false negatives, and 8 false positives, resulting in a sensitivity of 89.5% (95% confidence interval [CI], 66.9–98.7), a specificity of 55.6% (95% CI, 30.8–78.5), a positive predictive value of 68.0% (95% CI, 46.5–78.5), a negative predictive value of 83.3% (95% CI, 51.6–98.0), and an overall accuracy of 72.9% (95% CI, 55.9–86.2). Of the 8 false positives, 5 occurred during the first half-year after treatment. In our series,  $^{18}\text{F}$ -FDG PET provided significant clinical information in 18 of our 37 patients. This information included the exclusion of viable tumors in questionable lesions seen on MRI in 10 patients, the revealing of unexpected small metastatic lymphadenopathy in 3, and the disclosing of distant metastatic foci in 5. On the other hand,  $^{18}\text{F}$ -FDG PET provided no additional significant information to that provided by MRI in 9 patients. It even caused additional perplexity to the patients or extra cost for the confirmatory examinations in 10 patients, because of false-positive findings in 8 and false-negative findings in 2.

#### DISCUSSION

NPC is very radiosensitive, and most NPC tumors regress within 3 mo after radiotherapy. A persistent tumor is defined as a tumor that does not regress completely in 6 mo, and tumor recurrence is defined as a lesion detected after a documented tumor-free period (30). Detection of early recurrence is important because it can allow for the prompt institution of appropriate therapy (31).

Recurrent NPC is generally evaluated by conventional methods including physical examination, CT, and MRI. However, these methods may be compromised by granulation, fibrosis, tissue edema, and necrosis.  $^{18}\text{F}$ -FDG PET can identify viable tumor on the basis of higher glycolytic rates in neoplasms than in necrotic or reactive tissues. Therefore, it may have great potential in detecting recurrent NPC when the MRI findings are uncertain. To the best of our knowledge, only 2 studies using both  $^{18}\text{F}$ -FDG PET and MRI in the evaluation of recurrent NPC have been reported (27,28). Both had no false-negative results and a few false-positive results at the primary site, resulting in sensitivity of 100% and specificities of 93.4% and 92.9%. In another 3 papers concerned with  $^{18}\text{F}$ -FDG PET and CT of recurrent NPC at the primary site—studies by Kao et al. (24–26)—the sensitivity and specificity of  $^{18}\text{F}$ -FDG PET were 100% and 96%, respectively. However, such excellent results for  $^{18}\text{F}$ -FDG PET were not reproduced in the present work. In this series of 37 patients,  $^{18}\text{F}$ -FDG PET showed 1 false negative and 6 false positives at primary sites, resulting in a sensitivity of 91.6% and a specificity of 76.0%.

The published literature suggests that  $^{18}\text{F}$ -FDG PET is more specific than MRI or CT in detecting residual or recurrent nodal metastasis in head-and-neck malignancies, with sensitivities ranging from 67% to 100% and specificities ranging from 77% to 100% (19,21,22). However, to our knowledge, there have been no papers documenting

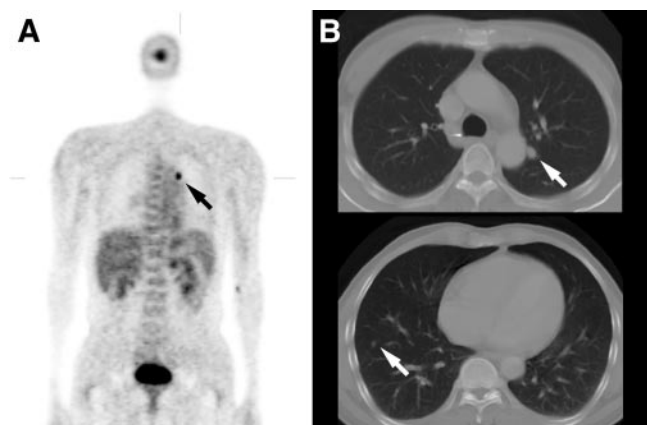


**FIGURE 5.** A 45-y-old woman with NPC 12 mo after concurrent chemoradiation therapy. (A)  $^{18}\text{F}$ -FDG PET scan shows an area of uptake (arrow) in the left hilar region. (B) Chest CT scan shows a small pulmonary nodule (arrow, top) in the left upper lobe and discloses another tiny nodule (arrow, bottom) in the right lower lobe. A follow-up CT scan 2 mo later showed definite enlargement at these 2 lung nodules, consistent with lung metastases.

such a role for  $^{18}\text{F}$ -FDG PET in NPC. In our series, the sensitivity and specificity of  $^{18}\text{F}$ -FDG PET in this regard were 90.0% and 88.9%, respectively, supporting the assertion that  $^{18}\text{F}$ -FDG PET should be a sensitive tool in detecting residual or recurrent nodes in NPC.  $^{18}\text{F}$ -FDG PET was particularly useful in 3 of our patients for whom MRI findings in the neck were negative but metastatic adenopathy was revealed by  $^{18}\text{F}$ -FDG PET. However, because 3 false-positive results were also found in our series, further diagnostic procedures should be pursued to avoid overstaging of recurrent disease. PET has been considered to have limitations for detection of nodal micrometastases and of tiny or necrotic metastatic nodes (19). Our single false-negative  $^{18}\text{F}$ -FDG PET result occurred in a patient with a small, residual high jugular node of 0.5-cm diameter.

Recurrent NPC may also develop at distant sites. Distant metastasis as the sole manifestation of recurrent disease, without locoregional recurrence, is rare (30) but did occur in 2 of our patients. Because  $^{18}\text{F}$ -FDG PET can easily scan the whole body, it has another advantage—that of disclosing unexpected tumor recurrence outside the head-and-neck region.  $^{18}\text{F}$ -FDG PET is particularly helpful if it averts the need for aggressive salvage treatment by early detection of distant metastases. However,  $^{18}\text{F}$ -FDG uptake at distant sites must be viewed with caution, as 3 of the 8  $^{18}\text{F}$ -FDG PET-positive scans in this series were false positive, including granulomatous axillary adenitis, reactive mediastinal nodal hyperplasia, and a posttraumatic effect in the humerus in 1 patient each. Also, of 5 patients with true-positive results for distant metastasis,  $^{18}\text{F}$ -FDG PET underestimated the number of lung metastases in 1 because of small size (Fig. 5). Although the sensitivity of  $^{18}\text{F}$ -FDG PET for distant metastases did not change on a patient-by-patient basis, it did change in terms of the number of metastatic foci, indicating that conventional cross-sectional imaging should be done to confirm the exact anatomic location and full extent of the  $^{18}\text{F}$ -FDG PET findings.

$^{18}\text{F}$ -FDG PET is an expensive modality and requires judicious use. Its role in the management of patients who have undergone therapy for NPC should be validated. Our prospective study showed that the overall sensitivity of  $^{18}\text{F}$ -FDG PET was high but the specificity was only moderate for detecting recurrent NPC. The high sensitivity to residual or recurrent disease is useful because, by aiding early detection, it enables timely institution of appropriate management. When  $^{18}\text{F}$ -FDG PET results are negative, our experience shows a high probability that patients have no residual or recurrent disease. However,  $^{18}\text{F}$ -FDG PET should not be substituted entirely for biopsy, as false-negative  $^{18}\text{F}$ -FDG PET results did occur in 2 of our patients. The reduced specificity in these data could be related to referral bias in this group with questionable MRI findings. Use of maximum-intensity-projection images for interpretation could be another cause of false-positive readings. Of note, a majority of false positives occurred during the early posttherapy period, suggesting the need for caution when

using PET earlier than 6 mo after treatment. Because the mean SUV of our true-positive lesions at the primary site was significantly higher than that of the false-positive lesions, SUV was a useful accessory reference to assist visual interpretation. However, both true-positive and false-positive uptake had a wide range of SUVs, and these partially overlapped with each other; thus, lesion-by-lesion differentiation could not entirely be based on a single SUV figure. The usefulness of SUV semiquantification at the regional nodes and distant sites was even less, because the difference in SUVs between true-positive and false-positive lesions was insignificant. A dual-phase technique was ordered in an attempt to enhance the diagnostic accuracy of visual interpretation. However, from the results in Table 3, it appeared to be unhelpful in such treated NPC patients and even resulted in more false positives. The moderate specificity may be associated with the additional costs of unnecessary conventional cross-sectional imaging or biopsy, and the clinician should be well aware of this problem. In our series, the false-positive rates for  $^{18}\text{F}$ -FDG PET of primary, nodal, and distant sites were 35.3%, 25%, and 37.5%, respectively. In clinical practice,  $^{18}\text{F}$ -FDG PET may be most useful in cases in which MRI findings are questionable but PET findings are true negative, or in which  $^{18}\text{F}$ -FDG PET reveals unexpected true-positive lesions not seen on MRI. In our series,  $^{18}\text{F}$ -FDG PET provided such useful information in 18 of our 37 patients. This information included true-negative results in 10 patients, revelation of unexpected small metastatic adenopathy in 3, and disclosure of distant metastatic foci in 5.

## CONCLUSION

Documentation of the performance of  $^{18}\text{F}$ -FDG PET for detecting recurrent NPC at primary, nodal, and distant sites can determine its clinical usefulness in this situation. Our results showed that  $^{18}\text{F}$ -FDG PET has a high sensitivity, but only a moderate specificity, for the detection of recurrent NPC in patients with equivocal MRI findings. Questionable MRI findings for tumor recurrence can better be characterized after  $^{18}\text{F}$ -FDG PET. Negative  $^{18}\text{F}$ -FDG PET findings virtually, although not absolutely, exclude tumor recurrence. Also,  $^{18}\text{F}$ -FDG PET contributes to the detection of unexpected nodal or distant metastatic foci. However,  $^{18}\text{F}$ -FDG PET suffers in specificity for recurrent tumor because it is sensitive to both tumor and inflammation. Overall,  $^{18}\text{F}$ -FDG PET appeared to provide additional significant information for about half of our NPC patients whose MRI studies showed questionable tumor recurrence.

## ACKNOWLEDGMENTS

We gratefully acknowledge grants from the National Science Council of Taiwan (NSC 92-2314-B-182A-081) and from the Chang Gung Memorial Hospital (CMRPG-32034 and CMRPG-32039).

## REFERENCES

- Simon MJ, Shanmugaratnam K, eds. The biology of nasopharyngeal carcinoma. In: *UICC Technical Report Series*. Geneva, Switzerland: International Union Against Cancer; 1982:17.
- Huang DP. Epidemiology and aetiology. In: Hasselt CAV, Gibb AG, eds. *Nasopharyngeal Carcinoma*. Hong Kong, China: The Chinese University Press; 1991:23.
- Parkin DM, Whelan DL, Ferley J. *Cancer Incidence in Five Continents*. Vol 7. Lyon France: International Agency for Research on Cancer; 1997. Publication 143.
- Easton JE, Levin PH, Hyarns VJ. Nasopharyngeal carcinoma in the United States: a pathological study of 177 US and 30 foreign cases. *Arch Otolaryngol*. 1980;106:88–91.
- Orecchia R, Airoidi M, Sola B, et al. Results of chemotherapy plus external re-irradiation in the treatment of locally advanced recurrences of nasopharyngeal carcinoma. *Eur J Cancer B Oral Oncol*. 1992;28B:109–111.
- Dimery IW, Peter LJ, Goepfert H, et al. Effectiveness of combined induction chemotherapy and radiotherapy in advanced nasopharyngeal carcinoma. *J Clin Oncol*. 1993;11:1919–1928.
- Lell M, Baum U, Gress H, et al. Head and neck tumors: imaging recurrent tumor and post-therapeutic changes with CT and MRI. *Eur J Radiol*. 2000;33:239–247.
- Ng SH, Liu HM, Ko SF, et al. Posttreatment imaging of the nasopharynx. *Eur J Radiol*. 2002;44:82–95.
- Becker M, Schroth G, Zbaren P. Long-term changes induced by high-dose irradiation of the head and neck region: imaging findings. *Radiographics*. 1997; 17:5–26.
- Chong VFH, Fan YF. Detection of recurrent nasopharyngeal carcinoma: MR imaging versus CT. *Radiology*. 1997;202:463–470.
- Olmi P, Fallai C, Colagradne S, Giannardi G. Staging and follow up of nasopharyngeal carcinoma: magnetic resonance imaging versus computerized tomography. *Int J Radiat Oncol Biol Phys*. 1995;32:795–800.
- Gong QY, Zheng GL, Zhu HY. MRI differentiation of recurrent nasopharyngeal carcinoma from postradiation fibrosis. *Comput Med Imaging Graph*. 1991;15: 423–429.
- Fujii M, Kanzaki J. The role of MRI for the diagnosis of recurrence of nasopharyngeal cancer. *Auris Nasus Larynx*. 1994;21:32–37.
- Ng SH, Chang TC, Ko SF, Wan YL, Tang LM, Chen WC. MRI in recurrent nasopharyngeal carcinoma. *Neuroradiology*. 1999;41:855–862.
- Ng SH, Wan YL, Ko SF, Chang JT. MRI of nasopharyngeal carcinoma with emphasis on relationship to radiotherapy. *J Magn Reson Imaging*. 1998;8:327–336.
- Ng SH, Chong VFH, Ko SF, Mukherji SK. Magnetic resonance imaging of nasopharyngeal carcinoma. *Top Magn Reson Imaging*. 1999;10:290–303.
- Wahl RL. Targeting glucose transporters for tumor imaging: “sweet” idea, “sour” result. *J Nucl Med*. 1996;37:1038–1041.
- Lapela M, Greneman R, Kurki T, et al. Head and neck cancer: detection of recurrence with PET and 2-[F-18] fluoro-2-deoxy-D-glucose. *Radiology*. 1995; 197:205–211.
- Fischbein NJ, Assar OS, Caputo GR, et al. Clinical utility of positron emission tomography with <sup>18</sup>F-fluoro-deoxyglucose in detecting residual/recurrent squamous cell carcinoma of head and neck. *AJNR*. 1998;19:1189–1196.
- Anzai Y, Carroll WR, Quint DJ, et al. Recurrence of head and neck cancer after surgery or irradiation: prospective comparison of 2-deoxy-2-[F-18]fluoro-D-glucose PET and MRI diagnoses. *Radiology*. 1996;200:135–141.
- Wong WL, Chevetron EB, McCurk M, et al. A prospective study of PET-FDG imaging for the assessment of head and neck squamous cell carcinoma. *Clin Otolaryngol*. 1997;22:209–214.
- Hanasono MM, Kunda LD, Segall GM, Ku GH, Terris DJ. Uses and limitations of FDG positron emission tomography in patients with head and neck cancer. *Laryngoscope*. 1990;109:880–885.
- Kao CH, Hsieh JF, Tsai SC, et al. Comparison of <sup>18</sup>F-2-fluoro-2-deoxyglucose positron emission tomography and computed tomography in detection of cervical lymph node metastases of nasopharyngeal carcinoma. *Ann Otol Rhinol Laryngol*. 2000;109:1130–1134.
- Kao CH, ChangLai SP, Chieng PU, Yen RF, Yen TC. Detection of recurrent or persistent nasopharyngeal carcinomas after radiotherapy with 18-fluoro-2-deoxyglucose positron emission tomography and comparison with computed tomography. *J Clin Oncol*. 1998;16:3550–3555.
- Kao CH, Tsai SC, Wong JJ, Ho YJ, Yen RF, Ho ST. Comparing <sup>18</sup>F-2-fluoro-2-deoxyglucose positron emission tomography with a combination of technetium 99m tetrofosmin single photon emission computed tomography and computed tomography to detect recurrent or persistent nasopharyngeal carcinomas after radiotherapy. *Cancer*. 2001;92:434–439.
- Kao CH, Shiau YC, Shen YY, Yen RF. Detection of recurrent or persistent nasopharyngeal carcinomas after radiotherapy with technetium-99m-methoxyisobutylisonitrile single photon emission computed tomography and computed tomography: comparison with 18-fluoro-2-deoxyglucose positron emission tomography. *Cancer*. 2002;94:1981–1986.
- Tsai MH, Shiau YC, Kao CH, Shen YY, Lin CC, Lee CC. Detection of recurrent nasopharyngeal carcinomas with positron emission tomography using 18-fluoro-2-deoxyglucose in patients with indeterminate MRI findings after radiotherapy. *J Cancer Res Clin Oncol*. 2002;128:279–282.
- Yen RF, Hung RL, Pan MH, et al. FDG PET in detecting residual/recurrent NPC and comparison with MRI. *Cancer*. 2003;98:283–287.
- Yen TC, Ng KK, Ma SY, et al. Value of dual-phase 2-fluoro-2-deoxy-D-glucose positron emission tomography in cervical cancer. *J Clin Oncol*. 2003;21:3651–3658.
- Sham JST, Wei WI, Kwan WH, Chan CW, Kwong WK, Choy D. Nasopharyngeal carcinoma: pattern of tumor regression after radiotherapy. *Cancer*. 1990;65: 216–220.
- Chang JT, See LC, Liao CT, et al. Locally recurrent nasopharyngeal carcinoma. *Radiation Oncol* 2000;54:135–142.